

HIGH RESOLUTION EXPERIMENTAL AND COMPUTATIONAL METHODS FOR MODELLING MULTIPLE ROW EFFUSION COOLING PERFORMANCE

A. V. Murray¹, P. T. Ireland¹, T. H. Wong¹, S. W. Tang¹, A. J. Rawlinson²

¹ Department of Engineering Science, University of Oxford, Parks Road, Oxford, UK, OX1 3PJ

² Turbine Systems, Rolls-Royce PLC, Derby, UK, DE24 8BJ

ABSTRACT

The continuing rise in turbine entry temperatures has necessitated the development of ever-more advanced cooling techniques. Effusion cooling, which is characterised by a high density of film holes operating at low blowing ratios, represents one possible mechanism for achieving high overall cooling effectiveness.

This paper presents an experimental investigation performed on flat-plate, effusion-type cooling geometries (with primary hole pitches of 3.0D and 5.75D) using pressure sensitive paint to yield high-resolution film effectiveness distributions using the heat/mass transfer analogy. CFD was used to model the setup computationally, with results comparing favourably to the experiments. The CFD domain was then altered to model a single hole. A superposition method was developed and applied to the two dimensional film effectiveness distribution, yielding data for an array of closely-packed holes. The method produced satisfactory results at higher pitches, but at lower pitches, high levels of jet interactions reduced the performance of the superposition method.

KEYWORDS

Effusion Cooling, Heat Transfer, Turbine Cooling, Pressure Sensitive Paint, Superposition

NOMENCLATURE

| | | | |
|---------------|--|-----------|-----------------------------|
| <i>C</i> | Mass Fraction | | Greek Characters |
| <i>D</i> | Diameter (<i>m</i>) | η_f | Film Effectiveness |
| <i>HP</i> | High Pressure | ρ | Density (kg/m^3) |
| <i>M</i> | Blowing Ratio, $(\rho_c V_c / \rho_\infty V_\infty)$ | | |
| <i>P</i> | Non-Dimensional Pitch | | Subscripts |
| p_{O_2} | Partial Pressure of Oxygen | <i>aw</i> | Adiabatic Wall |
| <i>PSP</i> | Pressure Sensitive Paint | <i>c</i> | Coolant Condition |
| <i>S</i> | Pitch (<i>m</i>) | <i>e</i> | Exit Condition |
| <i>span</i> | Spanwise Component | <i>in</i> | Inlet Condition |
| <i>stream</i> | Streamwise Component | ∞ | Mainstream Condition |
| <i>T</i> | Temperature (<i>K</i>) | <i>w</i> | Wall |
| <i>TET</i> | Turbine Entry Temperature | | |
| <i>TKE</i> | Turbulent Kinetic Energy (<i>J/kg</i>) | | |
| <i>v</i> | Velocity (<i>m/s</i>) | | |

INTRODUCTION

The ongoing drive to increase turbine thermal efficiency and specific power output has resulted in a continuing increase in both TETs and pressure ratio. As a consequence, the last fifty years have seen temperatures at entry to the HP turbine rise by over 500 K (Broomfield et al., 1998) with turbine blade operating temperatures now in excess of the material's engineering limits. This has necessitated increasingly complex methods of internal convective cooling on the inside of the blade surface, and external film cooling which acts to shield the blade from the hotter core gas. However, it is noted that raising coolant flow rate is at the detriment of engine efficiency and, as a result, cooling systems which achieve high cooling effectiveness using little coolant volume are preferable (Ireland, 2012).

Effusion cooling technology presents one possible method whereby high cooling performance can be achieved whilst simultaneously reducing the required coolant flow rate. It is fundamentally based upon a similar mechanism to film cooling in which coolant is passed through holes in the blade surface forming a protective film of cooler air. However, in the case of film cooling, the discrete nature and relatively large spacing of the holes results in an incomplete coverage of the protective film. Additionally, the high momentum flux of the jets through the film holes results in jet lift-off at the exit of the holes consequently increasing mixing losses and reducing cooling performance until the jets re-attach downstream (Krewinkel, 2013).

Effusive cooling systems differ from those of film cooling in the size and spacing of the holes, where effusion cooling is typically characterised by smaller diameter holes with a much smaller pitch than film cooling holes. This is often described by small non-dimensional hole pitch (S/D). This increased hole density with reduced diameter has been shown to provide significant increases in effectiveness (see Andrews et al. (1985), Gustafsson & Johansson (2001) and Crawford et al (1980)); this is a result of both a reduction in blowing ratio (and consequently jet lift-off) allowing the formation of a near continuous film, along with an increased convective effect within each of the cooling holes. Foster and Lampard (1980) demonstrated the rise in effectiveness with smaller spanwise hole pitching and also observed a decrease in jet lift-off. Relative to conventional films, variations in surface temperature are also reduced as hole density is increased (Gustafsson, 2001) and this can help alleviate thermal stresses that can have an adverse effect on blade life. As with film cooling, diffuser-shaped outlet holes are sometimes used to reduce jet exit velocity and help increase film coverage (Krewinkel, 2013). For similar reasons effusion holes are often inclined to the blade surface direction, typically at around 30-35° (Baldauf et al. (1999)). Hu and Ji (2004) performed a conjugate CFD study investigating the effect of varying inclination angle on cooling effectiveness and observed little variation in film performance between 30° and 60° inclined cylindrical holes. However, given the increased length for convective cooling with the 30° holes, this configuration is preferable. Krewinkel (2013) also discusses how variations in surface roughness due to manufacturing techniques have been shown to influence cooling performance with observations of greater roughness increasing effectiveness.

Challenges exist, however, in the successful implementation of effusion cooling systems which have, to-date, somewhat limited their application in gas turbine environments. As noted by Krewinkel (2013), manufacturing costs and concerns over component reliability remain, although advances in manufacturing methods are helping to address these issues. Additionally of consideration is the risk of blockage associated with the typically smaller hole diameters characteristic of effusion cooling. It is also noted that there exists an aerodynamic penalty associated with the mixing of film jets, and consequently, an optimisation process is required in the development of components to ensure that the thermal benefits of effusion type systems, outweigh any potential additional aerodynamic losses.

Experiments on effusion type systems have typically investigated non-dimensional hole pitches in the range of 2-15 (Cerri et al. (2007), Gustafsson & Johansson (2001), Manzhao et al. (2008) and Sweeney & Rhodes (1999)). However, to the best of the author's knowledge, few studies in the open literature have discussed and compared a range of computational and experimental methods for modelling multiple row effusion cooling performance.

The current study discusses a number of experimental and computational methods for modelling multi-row effusion cooling performance for two flat-plate effusion geometries utilising 30° inclined cylindrical cooling holes. The results of each method are then contrasted and discussed.

EXPERIMENTAL SETUP

The experimental study utilised one of the low speed wind tunnel facilities at the Osney Thermo-Fluids Laboratory (<http://www.eng.ox.ac.uk/thermofluids>), University of Oxford. A schematic of the experimental setup is provided in *Figure 1* with some of the key features elaborated on below.

The mainstream flow was comprised of ambient air, drawn in through a filtered open intake by a water ring vacuum pump, through a channel cross-sectional area measuring 192 mm × 24 mm. An upstream settling section was of sufficient length to allow flow development and help ensure a uniform velocity profile. All tunnel sections were manufactured from Perspex to allow for optical access.

Coolant flow comprised a mixture of air and nitrogen, the respective quantities of which were controlled by two automatic mass-flow controllers. The nitrogen source was a compressed nitrogen bottle whilst the coolant air supply was via the laboratory compressed air supply. Both gas streams were then mixed via a manifold system after which the mixed gas was passed through 4 hoses (of equal diameter and length) and entered the coolant plenum. To help ensure an even coolant feed, the 4 hoses were fed into the coolant plenum in a symmetrical manner and a two-layer perforated plate system used to dissipate the jets.

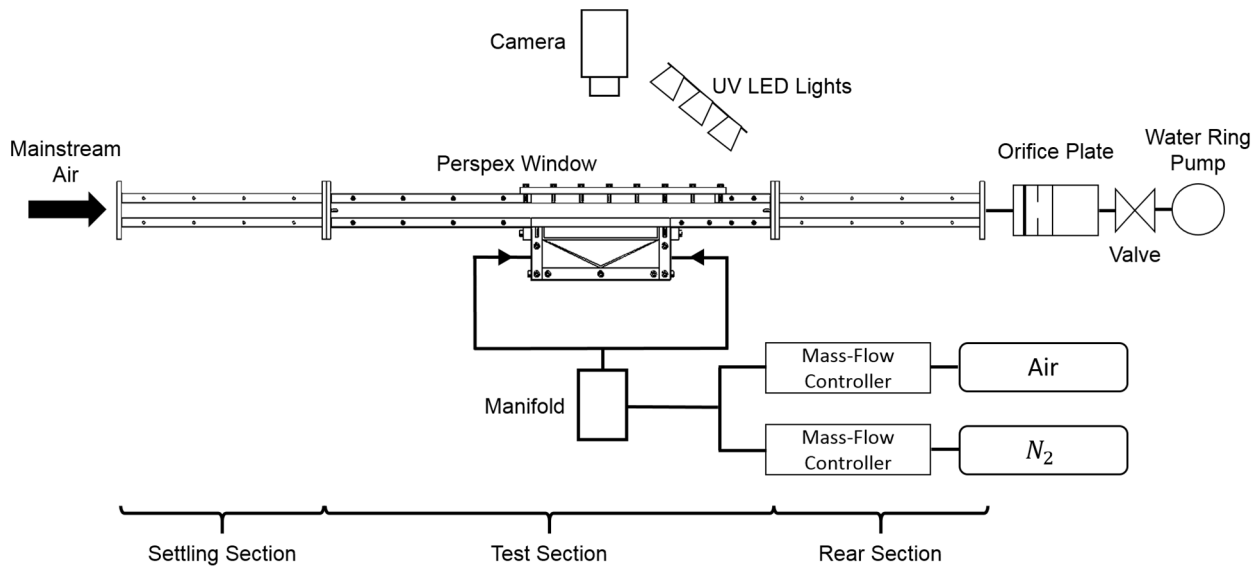


Figure 1 - Schematic of the experimental setup

Flat-Plate Effusion Cooling Geometries

The experimental setup was used to assess the film cooling performance achieved from two flat-plate cooling geometries. Both geometries exhibited a staggered configuration of circular film holes angled at 30° to the plate surface. Two non-dimensional hole pitches (based on the primary holes) were tested with geometry 1 exhibiting a pitch of $P_1 = 3.0$, and geometry 2 a pitch of approximately $P_2 = 5.75$. The hole diameter in both cases was 6.0 mm, and further plate dimensions are provided in *Figure 2*. It is also noted that geometry 1 exhibited a 7×8 array of primary holes with a total of 112 holes including those that were staggered, whilst geometry 2 exhibited a 4×5 array of primary holes with a total of 40 holes including the staggered hole components. The plates were manufactured from a single piece of aluminium of 2.5D depth with the holes drilled through the surface. O-ring seals

were placed at the base of the plates to minimise flow leakage during experiments with the plates being secured via bolts placed in each corner.

For both geometries, blowing ratios in the range of 0.1-1.2 were investigated. To achieve the required blowing ratio, both coolant and mainstream mass-flow rates were varied. Maximum mainstream inlet flow velocities were around 9.5 m/s, whilst to achieve the higher blowing ratios, mainstream inlet velocity was reduced to 5.75 m/s. It is noted that experimental errors increased at the lower blowing ratios given the precision of the mass-flow controllers however, these did not exceed 15%.

PSP Measurement Methodology

A brief overview of the PSP measurement technique is provided here, but the reader is referred to Wong et al. (2016), Gurram et al. (2016), and Han and Rallabandi (2010) for further details.

The UniFIB PSP used in the study is comprised of a mixture of Fluoro Isopropyl Butyl polymer (FIB), Platinum tetra (pentafluorophenyl) porphine (PtTFPP) and a white pigment. As noted by Wong et al. (2016), PtTFPP is a luminophore that responds when exposed to light of a certain wavelength. This response is quenched by interaction with oxygen, and consequently, the intensity of the emitted light decreases as the partial pressure of oxygen in contact with the PSP increases. By careful calibration, the partial pressure of oxygen can be determined at all positions across the PSP. The analogy of heat and mass transfer is fundamental to the experiment and consequently, the mainstream flow field was turbulent across all experiments. *Equation 1* demonstrates the experimental measurements of oxygen partial pressure required to allow for an estimation of film effectiveness by mass transfer analogy (Han and Rallabandi (2010)). Given the similar molecular weights of air and nitrogen, the mass fraction ratio is approximately equivalent to the mole fraction ratio and consequently the partial pressure ratio. It is also noted that in *equation 1* $C_{O_2,c}$ is zero as pure nitrogen was used as the coolant in the experiments.

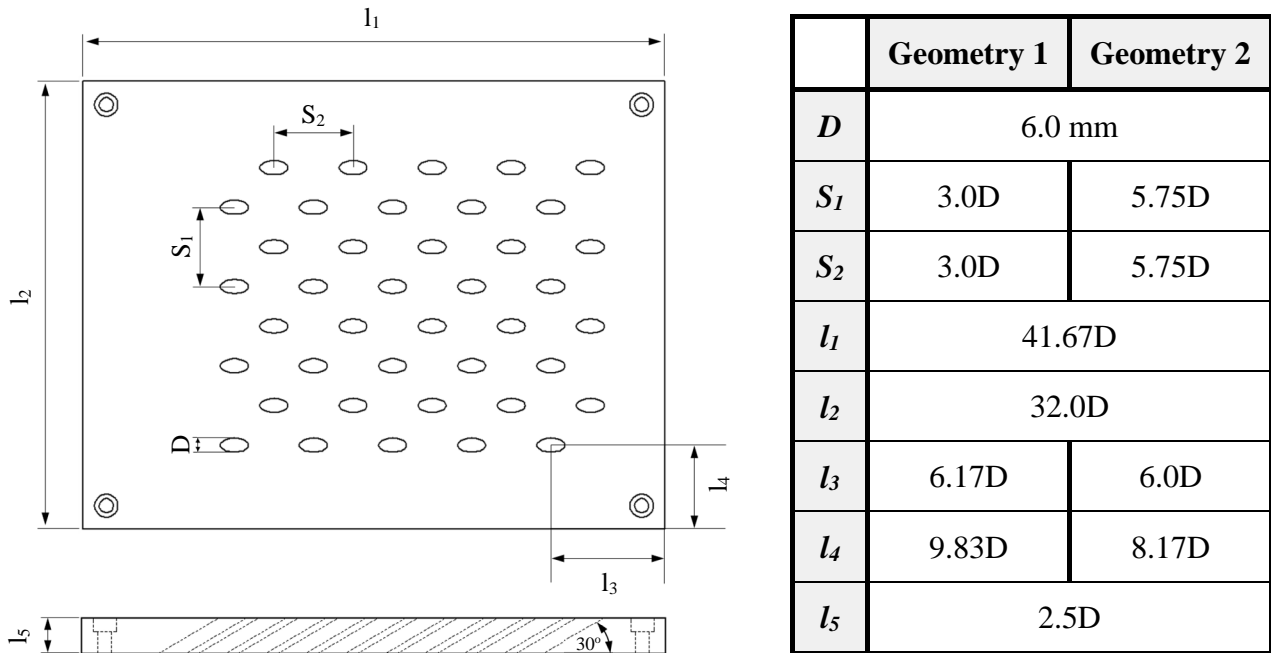


Figure 2 - Schematic showing the dimensions of the two flat-plate test geometries as a function of the film hole diameter

$$\eta_f = \frac{(T_\infty - T_{aw})}{(T_\infty - T_{c,e})} \approx \frac{(C_\infty - C_w)}{(C_\infty - C_c)} = \frac{(C_{O_2,air} - C_{O_2,N_2})}{(C_{O_2,air} - C_{O_2,c})} = 1 - \frac{C_{O_2,N_2}}{C_{O_2,air}} = 1 - \frac{p_{O_2,N_2}}{p_{O_2,air}} = 1 - \frac{p_{O_2,N_2}/p_{O_2,ref}}{p_{O_2,air}/p_{O_2,ref}} \quad (1)$$

During experiments a gas thermocouple was used to monitor coolant temperature with variations kept to a minimum in an attempt to reduce the impact of thermal effects on the PSP method. Intensity images of the experiments were captured using a 1928×1452 resolution, monochromatic CCD camera with a 610 nm long pass filter. The in-house *Matlab* post-processing method developed by Wong et al. (2016) was utilised in calculating film effectiveness from the raw image data. It is noted that, following the perturbation method discussed by Moffat (1988), the greatest uncertainty in film effectiveness values occur at lower effectiveness where for an effectiveness of around 0.14, the associated uncertainty is 3.1%. This drops to around 1.4% for effectiveness values greater than 0.8. For further details on the uncertainty associated with this PSP experimental rig setup, please see Wong et al. (2016) where this is discussed in greater detail.

COMPUTATIONAL SIMULATIONS

Modelling of film cooling performance by computational means provides a significant engineering challenge. Accurately capturing the innately complex flow features associated with film ejection and flow-mixing necessitate the use of dense computational meshes and more advanced turbulence models (such as those of LES) that require significant computational power. Indeed, CFD is well known to struggle with accurate prediction of absolute film effectiveness levels (Han (2013) and Kirollos & Povey (2015)). An alternative method of modelling film performance via CFD that was particularly suited to the validation of the PSP experimental results utilised a mass transfer method in which the concentrations of an introduced passive species was obtained throughout the flow domain. By heat-mass transfer analogy, the film effectiveness performance could be ascertained.

Multi-Hole CFD Domain and Setup

The multi-hole CFD simulations were performed using *Ansys Fluent* (version 16.2) on the same geometries as were tested in the experimental setup. The CFD domain modelled the test section used in the experimental setup. The mainstream flow domain commenced at the leading edge of the flat-plate with the exit of the simulated domain at the trailing edge of the plate. Viscous walls were situated at locations corresponding to the walls of the wind tunnel. Coolant was fed to the inlet of the effusion cooling holes via a plenum that was of identical cross-sectional area to the experimental setup. A velocity boundary condition was specified at the inlet of the mainstream flow with the velocity profile obtained from separate simulations that modelled flow development along the inlet settling section of the experimental rig. The coolant inlet boundary condition was a specified mass-flow rate. Both the mainstream and coolant boundary conditions were based upon the same values tested in the experiments. Additional boundary conditions were required for the introduced species at both flow inlets as well as the outlet. For both geometries a mesh refinement study was performed (using *Ansys ICEM*) to ascertain the required mesh fidelity to allow for relatively low simulation times whilst having little effect on the veracity of the results. Meshes for both geometries were approximately 6 million elements in size, were unstructured in nature and comprised of tetrahedral elements with prism layers at the solid/fluid interface and refinements around the film hole locations. In all simulations y^+ values were less than 5. Additionally, across all simulations the realisable $k-\epsilon$ turbulence model was used with enhanced wall treatment.

Single Hole CFD Domain, Setup and Superposition Method for Multi-Row Modelling

An additional method of effusion cooling modelling was considered which utilised the additive superposition method proposed by Sellers (1963). The use of a superposition model allows for the manipulation of data from a single film ejection to develop data for multi-row film performance. The Sellers model treats each ejected film as being an independent and confined layer and is described in *equation 2*. The basis of the method is that the freestream temperature for the single film cooling hole is replaced by the adiabatic wall temperature which results from the upstream films. To the authors' knowledge, the present work is the first to apply this process to detailed, two dimensional distributions of effectiveness.

$$\eta_f = 1 - \prod_{i=1}^n (1 - \eta_{f_i}(x)) \quad (2)$$

To make the method as comparable as feasibly possible to the experimental work and multi-hole CFD simulations, the CFD domain once again modelled the experimental setup, however, in this case the flat-plate simulated had only a single film hole. Mesh parameters and CFD solver setup remained the same as with the multiple hole simulations. After running the solution, the resulting film effectiveness distribution and node location information was imported into a bespoke *Matlab* script. The script replicated the film effectiveness data in the spanwise direction based on a specified hole pitch, whilst in the streamwise direction, the Sellers' superposition method was used to model downstream film development. For simplification, the non-dimensional pitching tested via this method was that of 5.75 given that there is little spanwise interaction between the individual films at this hole pitch. An example of the method is demonstrated in *Figure 3*.

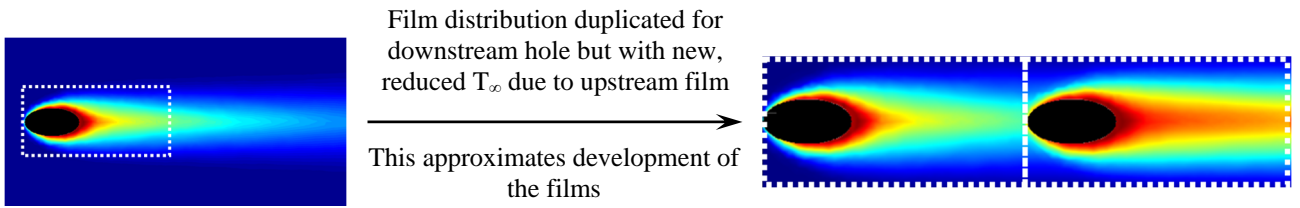


Figure 3 – Graphical demonstration of developed two dimensional superposition method (contour demonstrates film effectiveness)

RESULTS AND DISCUSSION

In the processing of all results, it is noted that data at the location of the film holes were set to *NaNs* and thus contained no data. Additionally, all methods of effusion modelling presented were for a density ratio of approximately unity. *Figure 4* depicts 2D adiabatic film effectiveness contours obtained from both the PSP experimental method and multi-hole CFD simulations at a range of blowing ratios for both geometries. Measurements were taken at blowing ratio increments of approximately 0.1 between the range of 0.1-1.2, but for brevity only a selection of the results are presented here.

Perhaps most striking are the highly effective films developed in the 3.0D pitch geometry. Given the close proximity of the holes, near continuous films are developed in which variations in spanwise effectiveness quickly diminish as blowing ratios are increased above 0.5, an effect that is captured in both the experiments and multi-hole CFD simulations. The results for this geometry also indicate that the number of rows of holes required for fully developed films is a strong function of the blowing ratio. Spanwise averaged results for the multi-hole CFD simulations (not shown here) indicate that for blowing ratios greater than 0.5, approximately 7 rows of primary holes are required for fully developed films – a value in keeping with observations made by Krewinkel (2013). Indeed, for blowing ratios between 0.5-1.2, little variation was observed in the spanwise averaged film effectiveness absolute values and trends.

The performance of the multi-hole, heat/mass transfer analogy CFD model for the 3.0D pitch geometry was reasonably satisfactory. Many of the trends captured in the experiments were evident in the CFD. At lower blowing ratios, there is a noticeable variation in film effectiveness across the spanwise holes in each row and this observed in both the CFD and PSP experiments. This is believed to result from variations in blowing ratio across the width of the test plate. Towards the edges of the plate, the development of the side-wall boundary layers act to reduce mainstream flow velocity; as a consequence, blowing ratio is increased at these edge film holes and the extent of the film cooling increased. The CFD over-predicts the performance of the films across all blowing ratios. The mixing of the jets observed in the CFD appears to be less than that shown by the experiments, and this is

evidenced by the reduced spreading of the films along with a slower rate of film decay. It is anticipated that the highly complex spanwise interactions between films ejected at the same row are not fully-resolved in the simulations and this accounts for some of variations observed between the CFD and experiments.

Good agreement was observed between the multi-hole CFD simulations and experimental results for the hole pitch of $5.75D$ and this is, in-part, expected to result from the reduced lateral jet interactions. The multi-hole CFD simulations capture the trends observed in the experiments particularly well with a steadily increasing film effectiveness up until a blowing ratio of

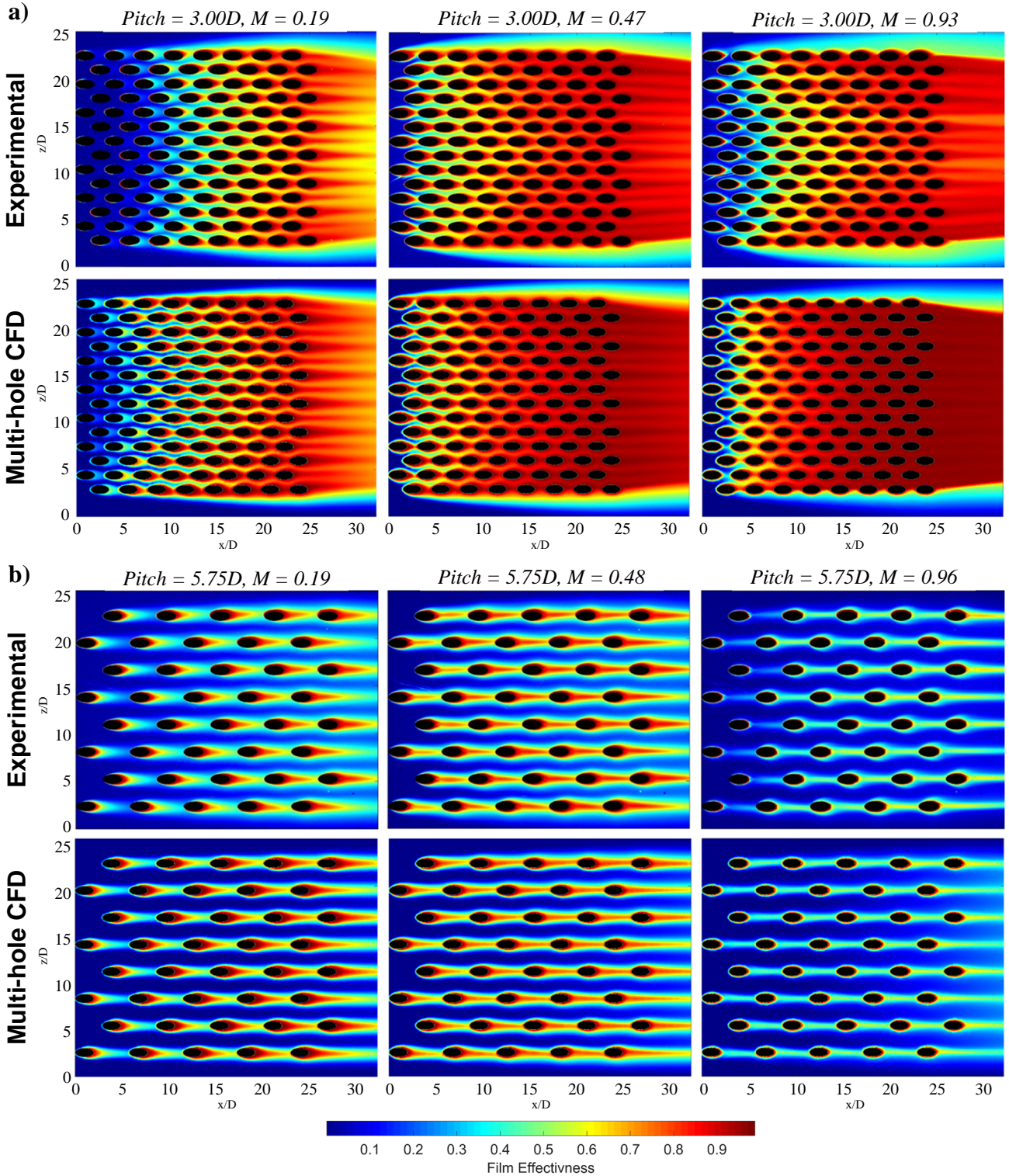


Figure 4 – PSP experimental and multi-hole CFD film effectiveness contours for three of the tested blowing ratios for non-dimensional hole pitches of a) 3.0 and b) 5.75

approximately 0.5, after which the effect of film lift-off is observed. As with the closer pitch geometry, the CFD does slightly under-predict mixing of the jets although this effect is relatively minimal. The number of primary hole rows required for fully-developed films also appears to be reduced when compared to the 3.0D geometry, with around 5 rows of holes being required (similar to observations made by Ling et al (2002)), although once again this is a function of blowing ratio. Furthermore, the multi-hole CFD model does appear to estimate a greater number of holes are required for fully-developed films and this effect increases with blowing ratios greater than 1 (see *Figure 7*).

To allow for further benchmarking of the results, the findings were compared to data obtained in a previous study by Ling et al. (2002) who attempted to quantify effusion cooling performance via a liquid crystal thermography method. Ling investigated two flat-plate geometries with hole pitches of 10D and 16D and presented the average film effectiveness achieved in the fully developed film region as a function of normalised coolant mass-flow. The data obtained by Ling has been adapted and is presented along with the data from the current study in *Figure 5*. The graph demonstrates the considerable increase in film effectiveness achieved with the closer pitched holes, with average film effectiveness in the fully developed region of the 3D pitch geometry between 0.8-0.9 across almost all blowing ratios investigated. The results therefore clearly demonstrate the potential of effusion cooling and the significant increases in cooling performance achieved at very low hole pitches at similar levels of coolant mass-flow.

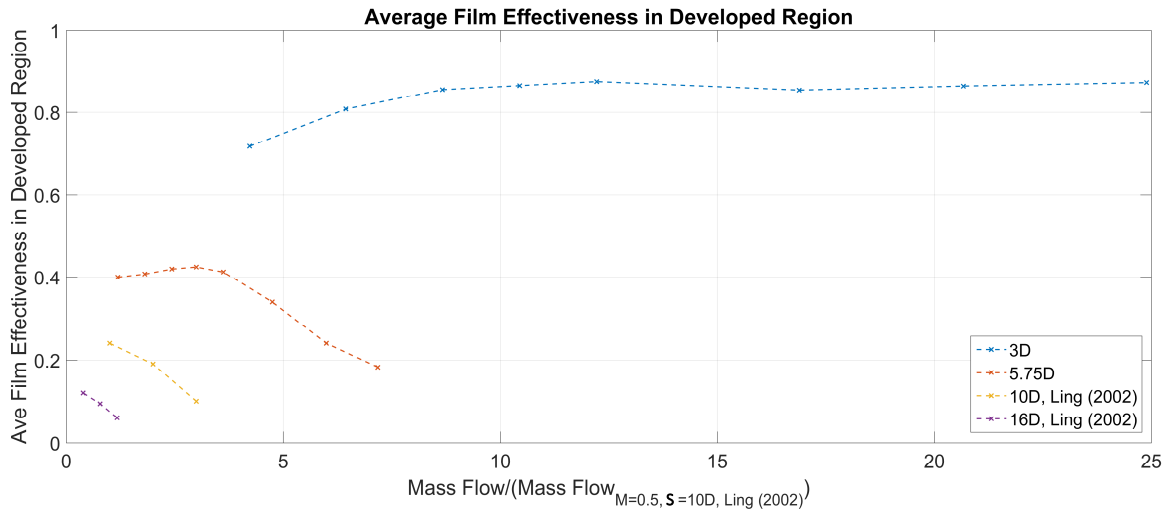


Figure 5 - Average film effectiveness in the developed film region against normalised mass-flow for both the 3D and 5.75D pitch geometries, along with a comparison against data obtained by Ling et al. (2002) for pitches of 10D and 16D

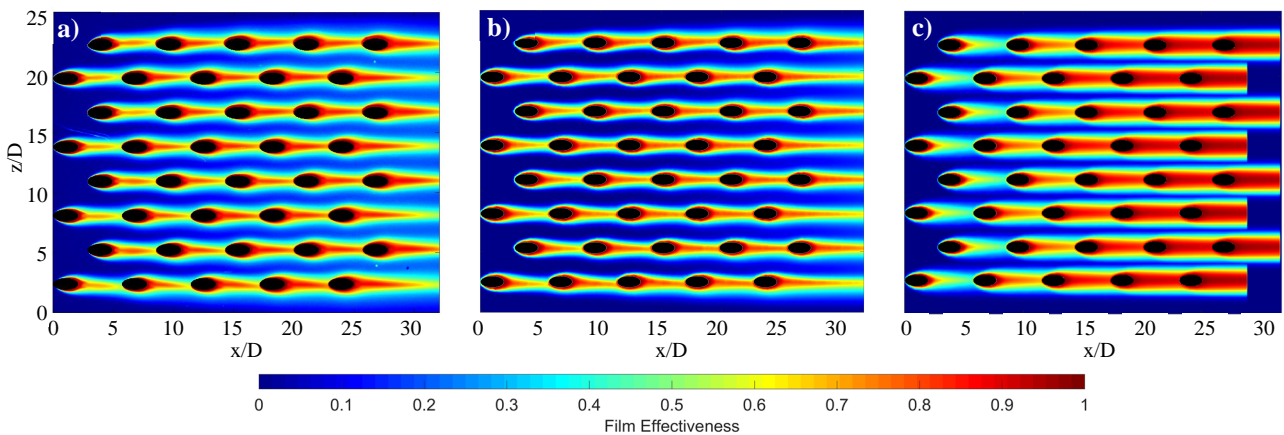


Figure 6 - Film effectiveness contours for a pitch of 5.75D and average blowing ratio of 0.48 from a) the PSP experimental rig, b) multi-hole CFD simulation, and c) Sellers' superposition method applied to a single hole CFD simulation using the two-dimensional film data

The Sellers' superposition method applied to a single hole CFD model displayed greater discrepancy when compared to the PSP experimental results and this is highlighted in *Figure 6*. The figure displays two dimensional film effectiveness data obtained from experiments and both the multi-hole and single-hole superposition CFD simulations at a blowing ratio of 0.48 on the 5.75D pitch geometry. Apparent is the considerable over-prediction in film development using the superposition method, with much wider and more effective films being developed by the second row of holes. This trend was observed across all blowing ratios tested with the deviation in effectiveness becoming more prominent as blowing ratio was elevated. This is well shown by *Figure 7* which displays spanwise averaged film effectiveness for three of the blowing ratios investigated using the experimental data, along with the results from both the computational methods.

Figure 7 demonstrates that, by a blowing ratio of approximately 1, spanwise averaged film effectiveness values via the superposition method were around twice those displayed by the multi-hole CFD simulation and PSP experiment. A number of reasons are hypothesised for this discrepancy. As already established, blowing ratio across the tested multi-hole plate was not constant and this is inherently disregarded in the superposition method. Effects of uneven flow turning in the coolant plenum which feeds the effusion holes was also evident in the multi-hole CFD model. This will once again effect both the blowing ratio and flow field in each individual hole and is not accounted for in the superposition method. The multi-hole CFD simulations also demonstrate how the upstream jets significantly impact the flow characteristics downstream with notable variations in both the velocity and turbulence profiles at downstream film holes. To further explore this hypothesis, further investigations were performed and are discussed below.

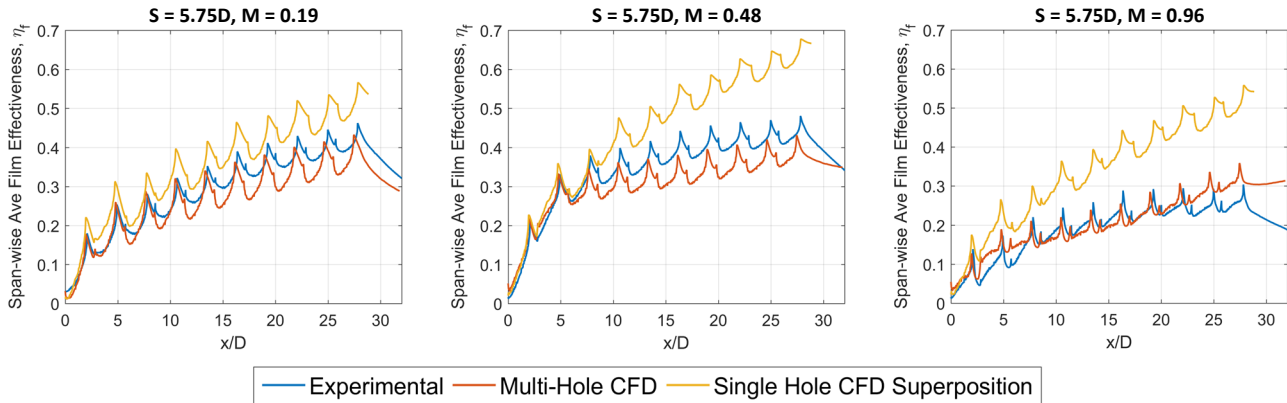


Figure 7 - Comparison of the spanwise averaged film effectiveness results for the PSP experiment, multi-hole CFD, and single hole superposition CFD model at three blowing ratios

Further Investigation of Superposition in Effusion Cooling Performance Modelling

To further investigate the cause of the significant deviation exhibited by the Sellers' superposition method in the above analysis, and to establish the applicability of the superposition method to effusion cooling, a further geometry was examined via the above multi-hole CFD method. Spanwise hole pitching in the geometry was maintained at 5.75D. To test the hypothesis that it is indeed the variations in the flow characteristics at downstream film holes caused by the upstream film jets, streamwise hole pitching was increased by a factor of three to 17.25D. It was anticipated, based on the previous results, that this hole pitching would allow for the re-establishment of the downstream flow-field and consequently minimise the effect of flow variations from upstream jets. It is noted that the CFD domain was extended to allow for three rows of primary holes to be simulated. In addition to the multi-hole CFD simulation, the superposition model was applied to the results from a single hole ejection and a comparison made. It is noted that for both methods of analysis, a blowing ratio of 0.48 was investigated and the coolant plenum domain adjusted so that each film hole inlet was fed separately allowing a blowing ratio of 0.48 to be maintained across each hole and consequently minimising the effect of small variations in M from each hole.

Figure 8 shows the resulting spanwise averaged film effectiveness plots for the increased hole pitch geometry for both the multi-hole CFD simulation and superposition method, along with the contour plots for each case. Apparent is the considerable improvement in the performance of the superposition method at increased streamwise hole pitching with peak spanwise averaged effectiveness values showing a less than 10% discrepancy by the third row of holes. The contour plots demonstrate that the superposition method still develops slightly stronger stripes of effectiveness, however, it is anticipated that this deviation would reduce as hole pitch is further increased. The results do indicate that at the low values of hole pitching that characterise effusion cooling, there are significant interactions between the film jets that act to reduce film effectiveness and these need to be accounted for in any superposition method.

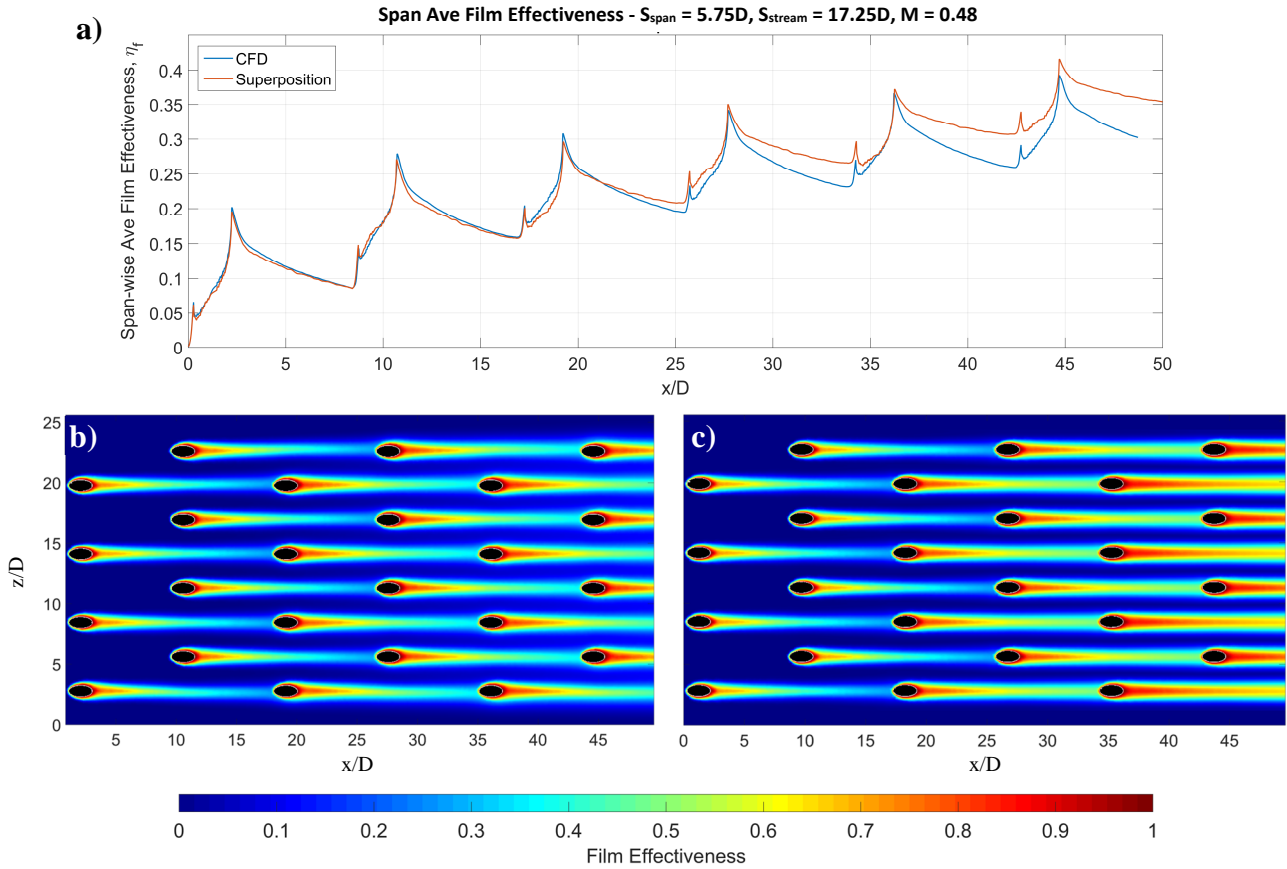


Figure 8 – a) Comparison of the spanwise averaged film effectiveness results from both the multi-hole CFD simulations and superposition method for the increased streamwise hole pitching of 17.25D (and spanwise of 5.75D) at a blowing ratio of 0.48, along with contour plots showing the film effectiveness trends from the b) multi-hole CFD simulation and c) superposition model

To further demonstrate the effect of upstream jet interactions, flow characteristics were compared for both the 5.75D and 17.25D streamwise hole pitch geometries for the case of a constant blowing ratio of 0.48 using the results of the CFD simulations. Contour plots depicting normalised velocity and turbulent kinetic energy at a height of 0.33D from the plate surface are demonstrated for both geometries in Figures 9 and 10 respectively. For the case of the 5.75D pitch geometry, there are notable interactions between upstream and downstream jets and these are clearly demonstrated in both the trends for velocity and TKE. Whilst the increased hole pitch still displays some interaction between jets, the effect is significantly reduced and the flow conditions prior to each hole are approximately the same. Thus, the cooling effect achieved from each hole is similar with little reduction in effectiveness being caused by increased turbulence and flow mixing from upstream jets. Consequently, it is suggested that, without alteration to the superposition method to account for

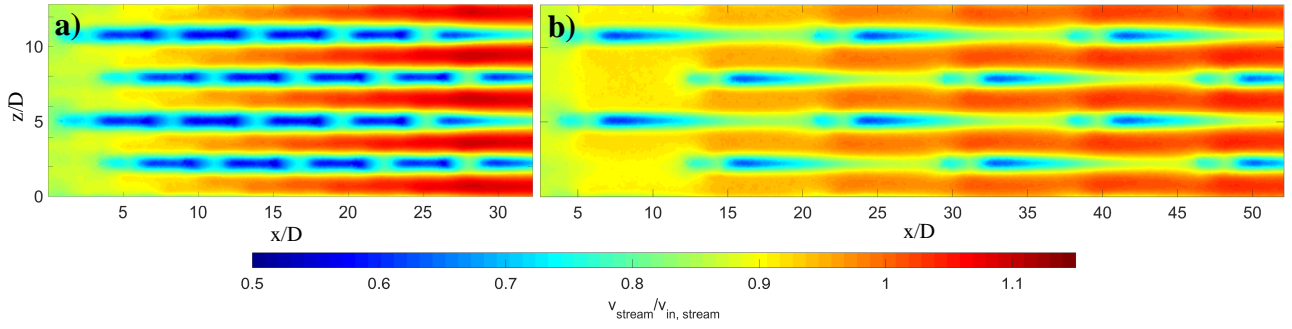


Figure 9 - Normalised streamwise velocity contours at a height of $0.33D$ from the plate surface for the streamwise hole pitches of a) $5.75D$ and b) $17.25D$ based on the results of the multi-hole CFD simulations

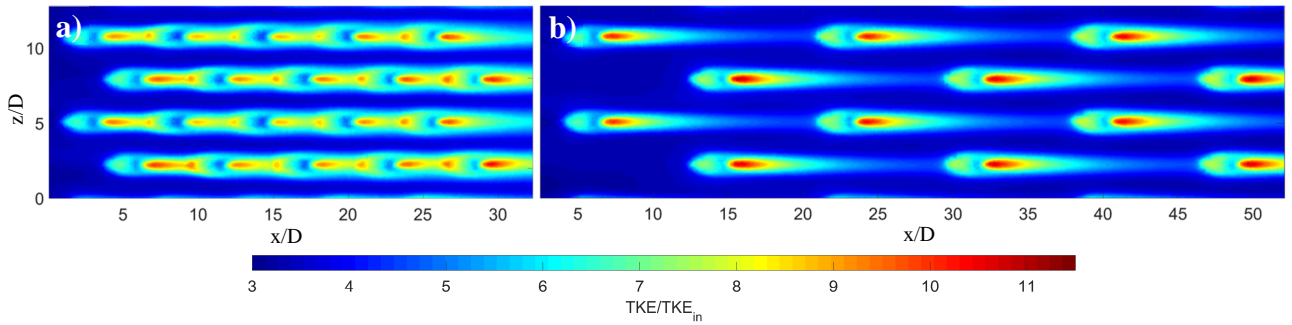


Figure 10 - Normalised turbulent kinetic energy contours at a height of $0.33D$ from the plate surface for the streamwise hole pitches of a) $5.75D$ and b) $17.25D$ based on the results of the multi-hole CFD simulations

variations in the flow field, its applicability to effusion cooling with closely pitched streamwise holes is somewhat limited.

CONCLUSIONS

The work presented in this paper has discussed a number of experimental and computational methods investigated for the modelling of multiple, staggered-row, effusion cooling geometries. Two flat-plate effusion cooling geometries were investigated with primary hole pitches of $3.0D$ and $5.75D$, at blowing ratios of between 0.1 - 1.2 .

The experimental PSP method developed has provided very high resolution effectiveness data that has permitted benchmarking of the computational methods. The experimental data has also demonstrated the very high values of film effectiveness that can be achieved at relatively low blowing ratios when utilising closely pitched, effusion cooling hole geometries. The $3.0D$ hole pitching geometry displayed strong spanwise jet interactions with near complete spanwise films being developed at blowing ratios as low as 0.3 . Whilst with the $5.75D$ pitch geometry, complete films were not developed at any of the investigated blowing ratios, the experimental results displayed strong film build-up in the streamwise direction.

The multi-hole, heat/mass transfer analogy CFD method has displayed promising results, particularly at the larger of the two pitches investigated in which both the trends observed and absolute film effectiveness values were very similar to those witnessed in the experiments. It is noted that the jet mixing displayed by the CFD does appear to under-predict those seen in the experiments, although this effect is less prominent at the larger pitching.

The results of the superposition model when applied to two dimensional film effectiveness distributions obtained from a single hole CFD simulation showed greater discrepancy with the experiments. This was primarily expected to result from the interactions between the jets primarily in the streamwise direction. Given the much closer hole pitching that characterises effusion cooling, these interactions are more significant. To test this hypothesis a further geometry was analysed which

maintained a spanwise pitch of $5.75D$, but increased the streamwise hole pitch by a factor of three to $17.25D$. The superposition method displayed much improved performance at this increased streamwise pitch. Indeed, the multi-hole CFD simulations demonstrated that at this greater hole pitch, the general flow field prior to each hole was approximately the same given the increased length over which the flow was able to re-establish after an upstream film ejection. This was displayed via streamwise velocity and turbulent kinetic energy contours that demonstrated the significant reduction in streamwise jet interactions when pitching was increased. Consequently, it is suggested that, in the case of effusion cooling, superposition methods need to take into account the complex jet interactions that result from the upstream film holes.

ACKNOWLEDGEMENTS

The authors wish to express their thanks for the on-going support provided by both Rolls-Royce plc and the EPSRC. The authors would also like to thank the technicians at the Osney Thermo-Fluids laboratory for their assistance in the manufacturing of the experimental setup.

REFERENCES

- Andrews, G. E., Asere, A. A., Gupta, M. L., & Mkpadi, M. C. (1985). Full coverage discrete hole film cooling: the influence of hole size. In *ASME 1985 International Gas Turbine Conference and Exhibit* (p. V003T09A003–V003T09A003). American Society of Mechanical Engineers.
- Baldauf, S., Schulz, A., & Wittig, S. (1999). High Resolution Measurements of Local Effectiveness by Discrete Hole Film Cooling.pdf. Presented at the International Gas Turbine & Aeroengine Conference & Exhibition, Indianapolis: American Society of Mechanical Engineers.
- Broomfield, R. W., Ford, D. A., Bhangu, J. K., Thomas, M. C., Frasier, D. J., Burkholder, P. S., Harris, K., Erickson, G. L., Wahl, J. B. (1998). Development and turbine engine performance of three advanced rhenium containing superalloys for single crystal and directionally solidified blades and vanes. *Journal of Engineering for Gas Turbines and Power*, 120(3), 595–608.
- Cerri, G., Giovannelli, A., Battisti, L., & Fedrizzi, R. (2007). Advances in effusive cooling techniques of gas turbines. *Applied Thermal Engineering*, 27(4), 692–698.
- Crawford, M. E., Kays, W. M., & Moffat, R. J. (1980). *Full-Coverage Film Cooling on Flat, Isothermal Surfaces: A Summary Report on Data and Predictions* (Contractor Report No. 3219) (p. 113). Stanford University: NASA.
- Foster, N. W., & Lampard, D. (1980). The Flow and Film Cooling Effectiveness Following Injection through a Row of Holes. *Journal of Engineering for Power*, 102(3), 584–588.
- Gurram, N., Ireland, P. T., Wong, T. H., & Self, K. P. (2016). Study of Film Cooling in the Trailing Edge Region of a Turbine Rotor Blade in High Speed Flow Using Pressure Sensitive Paint. In *ASME Turbo Expo 2016: Turbomachinery Technical Conference and Exposition* (p. V05CT19A023–V05CT19A023). American Society of Mechanical Engineers.
- Gustafsson, B. (2001). *Experimental Studies of Effusion Cooling* (Doctor of Philosophy Thesis). Chalmers University of Technology, Goteborg, Sweden.
- Gustafsson, K. M. B., & Johansson, T. G. (2001). An Experimental Study of Surface Temperature Distribution on Effusion-Cooled Plates. *Journal of Engineering for Gas Turbines and Power*, 123(2), 308.
- Han, J.-C. (2013). Fundamental gas turbine heat transfer. *Journal of Thermal Science and Engineering Applications*, 5(2), 021007.
- Han, J.-C., & Rallabandi, A. P. (2010). Turbine Blade Film Cooling Using PSP Technique. *Frontiers in Heat and Mass Transfer*, 1(1).

- Hu, Y., & Ji, H. (2004). Numerical study of the effect of blowing angle on cooling effectiveness of an effusion cooling. In *ASME Turbo Expo 2004: Power for Land, Sea, and Air* (pp. 877–884). American Society of Mechanical Engineers.
- Kirollos, B., & Povey, T. (2015). An Energy-Based Method for Predicting the Additive Effect of Multiple Film Cooling Rows. *Journal of Engineering for Gas Turbines and Power*, 137(12), 122607.
- Krewinkel, R. (2013). A review of gas turbine effusion cooling studies. *International Journal of Heat and Mass Transfer*, 66, 706–722.
- Ling, J. C., Ireland, P. T., & Turner, L. (2002). Full coverage film cooling for combustor transition sections. In *ASME Turbo Expo 2002: Power for Land, Sea, and Air* (pp. 1011–1021). American Society of Mechanical Engineers.
- Manzhao, K., Huiaren, Z., Songling, L., & Hepeng, Y. (2008). Internal heat transfer characteristics of lamilloy configurations. *Chinese Journal of Aeronautics*, 21(1), 28–34.
- Moffat, R. J. (1988). Describing the uncertainties in experimental results. *Experimental Thermal and Fluid Science*, 1(1), 3–17.
- Sellers, J. P. (1963). Gaseous Film Cooling With Multiple Injection Stations. *AIAA Journal*, 1(9), 2154–2156.
- Sweeney, P. C., & Rhodes, J. F. (1999). An infrared technique for evaluating turbine airfoil cooling designs. In *ASME 1999 International Gas Turbine and Aeroengine Congress and Exhibition* (p. V003T01A033–V003T01A033). American Society of Mechanical Engineers.
- Wong, T. H., Ireland, P. T., & Self, K. P. (2016). Film Cooling Effectiveness Measurements on Trailing Edge Cutback Surface and Lands Following Novel Cross Corrugated Slot Geometry (GT2016-57371). In *Proceedings of ASME Turbo Expo 2016*. Seoul, South Korea: American Society of Mechanical Engineers.